Nova Biotechnologica *et* Chimica

Treatment of produced water by induced air flotation: effect of both Tween 80 and ethanol concentrations on the recovery of PAHs

Salima Chebbi[1], Atmane Allouche[2,✉], Marian Schwarz[3], Souhila Rabhi[1], Hayet Belkacemi[1] and Djoudi Merabet[1]

[1]*Materials Technology and Process Engineering Laboratory, University of Bejaia, Targa Ouzemmour Road, Bejaia, 06000, Algeria*

[2]*Applied Hydraulics and Environment Research Laboratory, University of Bejaia, Targa Ouzemmour Road, Bejaia, 06000, Algeria*

[3]*Department of Environmental Engineering, Faculty of Ecology and Environmental Sciences, Technical University in Zvolen, T. G.Masaryka 24, Zvolen, SK-960 53, Slovak Republic*

Article info

Abstract

The present study investigates the application of induced air flotation (IAF) technique on PAHs (PAHs) removal performance from a real oilfield produced water of a separator cell. The quantification of total PAHs (PAH_{tot}) was done using ultraviolet-visible spectrometry (UV-Vis) according to the naphthalene calibration curve. The UV-Vis spectra of naphthalene dissolved in a mixture of the binary solvent (water-ethanol) and the Tween 80 showed stability in the molecular orbital of $C_{10}H_8$. The use of small concentration of Tween 80 was revealed to be discrete in the quantification of PAH_{tot}. The flotation process was improved at the critical micelle concentration of Tween 80 (CMC) of 2 % and the critical coalescence concentration of ethanol (CCC) of 0.5 mL/L for the PAH_{tot} recovery of 49.76 % and the PAH_{tot} content in the pulp of 50.24 %. At these concentrations, half of PAH_{tot} was removed from produced water PW. Above the CMC and the CCC, the PAH_{tot} recovery decreased and the PAH_{tot} content in the pulp increased. It was found that there is a collector concentration at which the amount of water carrying from the pulp to the concentrate was increased and in parallel, the PAH_{tot} recovery increased and the PAH_{tot} content in the pulp decreased. Both of the CMC and the CCC have promoted the decrease on the conditioning time from 30 to 10 min and the flotation time from 20 to 6 min. Since the impeller speed and air flow rate were constant, the flotation of PAHs was limited. The flotation kinetics of PAH_{tot} was described by the Higuchi model.

Introduction

Produced water (PW) represents the largest volume waste stream in oil and gas production operations (El-Kayar *et al.* 1993; Pardue *et al.* 2014). It is common that oil well production fluids in the old reservoirs are eventually composed of 90 % or more of water and only 10 % or less of hydrocarbons (Edwan and Qomarudin 2015). PW properties can even be varying throughout the lifetime of the reservoir (Alanezi *et al.* 2013; Akinwumi 2013; Hagström *et al.* 2016). Concentrations of total polycyclic aromatic hydrocarbons (PAH_{tot}), the main toxics and persistent in the marine environment (Fisner *et al.* 2013), typically range from about 0.040 to about

✉ *Corresponding author:* atmanea@gmail.com

3 mg/L (Lee and Neff 2011; Chebbi *et al.* 2016) and consist primarily of the most water-soluble congeners, the 2- and 3-ring PAH, such as naphthalene, phenanthrene (Lee and Neff 2011). Marine animals near a PW discharge may bioaccumulate PAHtot from the ambient water, their food, or bottom sediments (Lee and Neff 2011; Almeda *et al.* 2013). Therefore, it is important to treat the PW intended for sea disposal on the platform or at a shore treatment facility.

Induced air flotation (IAF) is an efficient process for removing various organic pollutants from PW (El-Kayar *et al*. 1993; Zheng and Zhao 1993; Painmanakul *et al.* 2010). According to its fundamental principles, very fine air bubbles have to be produced in the liquid to enable them to adhere to the hydrophobic particles and to float them to the surface (Sylvester and Byeseda 1980; Li and Tsuge 2006). The surface of the dispersed particles has to be hydrophobic by nature or be made hydrophobic by collectors (Wang *et al.* 2010). Tween series are known for their assistance in separating such pollutants such as hydrophobic organic compounds from water and soils (Hoseini *et al.* 2013; Lau *et al.* 2014; Roodbari *et al.* 2016; Gharibzadeh *et al.* 2016). Their low toxicity and acceptable degree of biodegradability are responsible for their extensive utility (Szymczyk and Taraba 2016). However, flotation process requires formation of a froth layer that is to some extent stable. Bubbles can collide and coalesce into larger bubbles but large bubbles are ineffective for flotation. They rise rapidly creating unfavorable turbulence and break-up of bubble-particle agglomerates (Moosai and Dawe 2003; Bournival *et al.* 2015. Literature studies indicated that the use of frothers increases air dispersion into fine bubbles, and reduces in coalescence of individual bubbles and decreases in the rate at which the bubbles rise to the surface (Gupta *et al.* 2007).

It is known that the flotation of particles is automatically accompanied by the recovery of water. Furthermore, as the formed bubbles are large, the amount of recovered water is important. Decreasing the amount of the entrained water is an important research issue in flotation process, since the large amounts of entrained water alter the oil quality. Moyo *et al.* (2007) reported that alcohol frother entrained less amount of water.

A key factor in effective flotation is strong attachment of the contaminant to the air bubble (Wang *et al.* 2010). Chemicals may be added to assist the attachment (Wang *et al.* 2010; Ofori *et al.* 2012). If there is such chemical intervention, the type of chemicals added, and their concentrations are important. If a full understanding of the physical processes can be gained by operators, the optimal conditions for a particular throughput and contaminant concentration reduction may be more successfully established. Thence operating efficiency may be increased, and costs minimized (Moosai and Dawe 2003).

In this research, ultraviolet–visible spectrometry (UV-Vis) was employed to probe the interaction of naphthalene and the binary solvent (water-ethanol). The effect of both Tween 80 and ethanol concentrations on the flotation of PAHs from a real oilfield PW were investigated. The flotation kinetics was studied through a kinetics experiment. First order kinetics and Higuchi models were applied to describe and evaluate the flotation of PAHs. UV-Vis spectrometry was investigated to quantify PAHtot. The main objectives of this study were to evaluate the IAF performance.

Experimental

Sites and sampling

The real oilfield PW was obtained from SONATRACH Company of Bejaia, Algeria. Samples were collected *in situ*, at the outlet of hydrocarbon storage tank, and stocked in amber glass bottles, in order to prevent the photodegradation of organic matters.

Chemicals

The hydrochloric acid (HCl) 35 – 37 % (*v/v*) and the nonionic collector (Tween 80) were obtained from Biochem Chemopharma, Montreal. Ethanol (C_2H_6O) 96 % (*v/v*) was obtained from Sigma-Aldrich. Naphthalene ($C_{10}H_8$) was obtained from Panreac Quimica SA (Spain).

Experimental setup

Tween 80 was used as a nonionic collector.

The frother employed was ethanol (at 96 %). Precise amounts of Tween 80 were dissolved in ethanol to produce a collector-frother solution. By varying the concentrations of Tween 80 in ethanol from 0.5 to 20 % and of the quantity of collector-frother solution from 0.2 to 1.5 mL added to the flotation cell, the effect of a wide range of Tween 80 and ethanol concentrations on the PAH$_{tot}$ recovery from PW by IAF could be tested.

Both of Tween 80 and 96 % ethanol solutions and mixture were prepared. Naphthalene in 96 % ethanol and a mixture of naphthalene, Tween 80 and 96 % ethanol were prepared at known dosages. These different systems were analyzed by UV-Vis spectrometry.

The flotation tests were conducted on a real oilfield PW using a laboratory type Denver flotation of 1 L capacity under the following conditions: Room temperature, pH 2, Impeller speed: 750 revolutions per minute (rpm), Conditioning time: 10 min Flotation time: 12 min. The pulp was introduced in the flotation cell of 1 L and was conditioned, during 10 min, with Tween 80-ethanol during 5 min after 5 min of stirring at an appropriate dosage. Air was introduced in the pulp by opening the air valve and the froth floated as a concentrate was collected during 12 min. The PAH$_{tot}$ recovery and its content in the pulp were determined using UV-Vis spectrometry analysis and then, optimal collector-frother concentrations were determined.

The flotation kinetics of PAH$_{tot}$ from a real oilfield PW at these optimal concentrations was studied. The flotation tests were done as following: after conditioning, air was injected; 2 mL of samples were taken from the froth each 2 min of flotation until the end of the process for two different condition times (5 and 10 min) and then, PAH$_{tot}$ concentrations were determined by UV-Vis spectrometry analysis.

Data Analysis

Measurement of PAH$_{tot}$ by UV-Vis spectrometry

Samples were centrifuged for 5 min at 6,000 rpm. The dilutions were made on 0.5 mL of samples and transferred into glass pill dispensers to which were added 0.5 mL of 96 % ethanol in order to form water-96 % ethanol mixtures (*v/v*) for analysis

by UV-Vis spectrometry, similarly it has been established the naphthalene calibration curve in water-96 % ethanol (*v/v*).

The calibration curve for naphthalene was established by obtaining optical densities on a series of dilutions made from the 100 mg/L solution in water-96 % ethanol mixture (*v/v*), at a wavelength of 220 nm (Mistry 2009) (coefficient of regression, R^2 = 0.999), measured on a SHIMADZU Spectrometer. Naphthalene is a hydrophobic compound with low solubility in water. Samples were calculated from concentration dosages determined from optical densities measured at a wavelength of 220 nm, on the calibration curve for naphthalene.

Concentration analysis was carried out for the recovered PAH$_{tot}$. Calculation of the PAH$_{tot}$ recovery was done as following (Lau *et al.* 2013), as in (Eq. 1):

$$\text{Rep} = \left[1 - \left(\frac{C_p * V_p}{C_i * V_i}\right)\right] \times 100 \text{ \%} \qquad (1)$$

where C_i and C_p: Concentrations of PAH$_{tot}$ in the PW and the pulp, respectively. V_i and V_p: Volumes of the PW and the pulp, respectively. Regression model of the data is obtained using Origin 6.0 scientific plotting software.

Kinetics

The mathematical description of the effect of both CMC and CCC on the flotation of PAH$_{tot}$ according to time can be represented by supposing the first-order kinetics and the Higuchi model (Ramaswamy *et al.* 2007; Siepmann and Peppas 2011).

$$\textit{First-order} \qquad \ln\left(\frac{C_t}{C_f}\right) = -kt \qquad (2)$$

where k (min^{-1}) is the flotation rate constant.

$$\textit{Higuchi model} \qquad \frac{C_t}{C_f} = K_H \, t^{0.5} \qquad (3)$$

K_H is the flotation rate constant for the Higuchi Model; C_t (mg/L) is the concentration of the PAH$_{tot}$ at any time and C_f (mg/L) is the final concentration of the PAH$_{tot}$ at the end of the flotation process above which PAH$_{tot}$ concentrations weren't appreciable.

The criterion for selecting the most appropriate model was based on a goodness-of-fit test. Regression model of the data is obtained using Origin 6.0 scientific plotting software.

Results and Discussion

UV-Vis analysis

PAH molecules are extremely stable in their neutral and ionized forms (Crawford and Tielens 1985; Salama and Allamandola 1995). UV-visible spectra of small PAHs (2 or 3 rings) show strong absorptions in the ultraviolet corresponding to the $\pi \rightarrow \pi^*$ transitions and exhibit characteristic absorption bands of conjugated aromatic bonds with considerable fine structure, centered at "B" band with less intensity at 276 nm, due to the associated of the electronic transition with the vibration movement which disturb the symmetrical structure of the aromatic cycle (Salama and Allamandola 1995). The second band more intense at 220 nm is due to the more rigid and symmetrical structure state of naphthalene (Salama and Allamandola 1992; Salama and Allamandola 1993; Salama and Allamandola 1995).

The UV–visible spectra were used for qualitative and quantitative analysis (Monakhova *et al.* 2010; Weide *et al.* 2015. Therefore by measuring the UV absorbance of a sample containing PAHs, one can quantify the total hydrocarbons (PAH$_{tot}$) which can be obtained *via* calibration (Lee and Neff 2007). A series of operations on data carried out on qualitative UV-visible analysis of 96 % ethanol and both naphthalene ($C_{10}H_8$) and Tween 80, in the same solvent; at known concentrations were established. UV spectra were recorded over the wavelength range of 200 – 400 nm using Single-Beam UV-visible Spectrometer (SpectroScan 30). Fig. 1 shows the UV spectra of 96 % ethanol, utilized as solvent, and $C_{10}H_8$ (1 mg/L) dissolved in 96 % ethanol. The reference solutions used during the scanning of both 96 % ethanol and $C_{10}H_8$ samples were water, 96 % and absolute ethanol, respectively. Data from the UV spectrum of 96 % ethanol (1) show that the absorption of ethanol of UV light ranges from 200 – 287 nm, with both a considerable and moderate decrease in absorption between 200 – 210 nm and 210 – 240 nm, respectively, until reaching a zero absorbance at 287 nm.

The full-scan UV detection of $C_{10}H_8$ sample in 96 % ethanol (2), with water as reference, shows
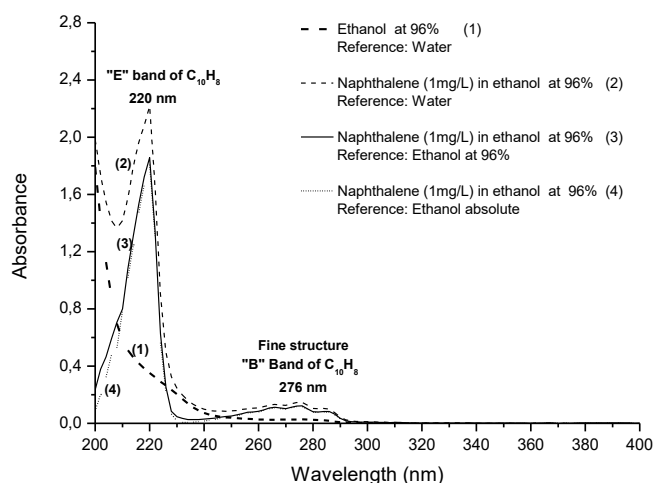

Fig. 1. UV spectra of naphthalene ($C_{10}H_8$) (1 mg/L) dissolved in 96 % ethanol.

in 96 % ethanol (2), with water as reference, shows the spectrum overlapping of ethanol absolute and $C_{10}H_8$ in the UV region where they absorb. Furthermore, the shape of the three spectra of $C_{10}H_8$ samples is similar and no solvent effect is observed on the absorption wavelengths, except for the existence of a shift of the spectrum (2) towards higher values of absorbance, compared with the spectra with respect to 96 % (Pardue *et al.* 2014) or absolute (4) ethanol. This difference is due to the absorption of ethanol with respect to water.

In accordance with the full-scan UV detection of both $C_{10}H_8$ samples and 96 % ethanol, the intensity of the reference beams have suffered no light absorption. Furthermore, the absorption spectra reveal that ethanol and water (polar solvents) did not destabilize the molecular orbital of $C_{10}H_8$ molecule. The obtained results show that despite the presence of the $C_{10}H_8$ molecules in a binary solvent (water-ethanol), the use of two or of one of them as reference did not influenced the shape of the obtained spectrum of the $C_{10}H_8$ molecules.
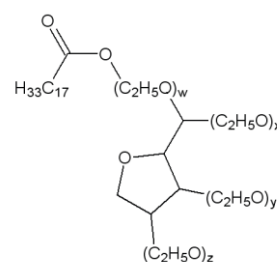
Fig. 2. Molecular structure of Tween 80. Indexes *x*, *y*, *z*, and *w* at chromophore groups were selected as 5 (Karjiban *et al.* 2012).
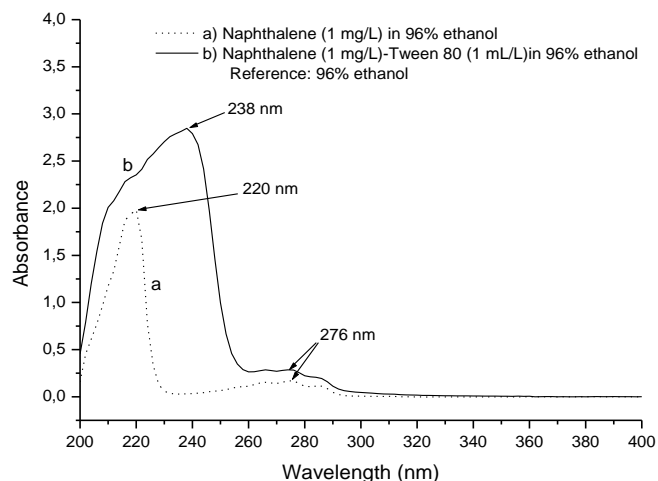
184
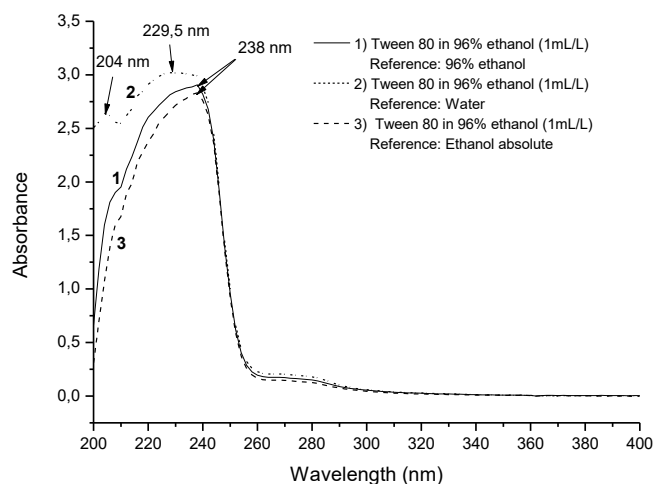
Fig. 3. UV spectra of Tween 80 (1 mL/L) dissolved in 96 % ethanol.

Fig. 4. UV spectra of: a) $C_{10}H_8$ (1 mg/L) and b) $C_{10}H_8$ (1 mg/L)-Tween 80 (1 mL/L) in 96 % ethanol.

The molecular structure of Tween 80 molecule (Fig. 2) is characterized by a chromophore group in their structure. It is an ester with system "π" (C=O) conjugated with the two electron "n" in the auxochrom group (oxygen of carboxylate in α position of carbonyle) corresponding to the n→π* transition; it absorbs in the UV range (Wuelfing *et al.* 2006). The UV absorption spectra (Fig. 3) of Tween 80 (1 mL/L) dissolved in 96 % ethanol were similar with both 96 % ethanol (1) and absolute ethanol (2) as reference solutions. The shapes of curves (obtained at 238 nm) suggest no effect of solvent.

For the absorption spectrum of Tween 80 (1 mL/L), with water as reference (2), we noticed two absorption bands. The first ranged from 200 – 210 nm and peaked at 204 nm, and the second ranged from 210 – 287 nm and peaked at 329.5 nm. The absorption band in the range of 200 – 210 nm is relative to ethanol, as shown in Fig. 1. Therefore, the choice of reference solution played an important role in both qualitative and quantitative analysis by molecular spectrometry.

The absorption spectra of $C_{10}H_8$ (1 mg/L), Tween 80 (1 mL/L) and $C_{10}H_8$-Tween 80 in 96 % ethanol, with 96 % ethanol as a reference, are shown in Fig. 4.

For $C_{10}H_8$ (1 mg/L): In the wavelength range covered in our experiments (200 – 400 nm), $C_{10}H_8$ shows two distinct band systems with very different intensities. System I, peaking at 220 nm, is very strong. System II is very weak and peaks at 276 nm. We also note that $C_{10}H_8$ may contribute

to the 220 nm bump (Salama and Allamandola 1992; Salama and Allamandola 1995). Studies carried out by Salama and Allamandola (1992) strongly attest that the continuum observed in the wavelength range of 200 – 232 nm is due to the neutral naphthalene ($C_{10}H_8$), and in the wavelength range of 232 – 296 nm is due to fine structure of naphthalene. Furthermore, there is one way in which one can examine the possible quantification of the $C_{10}H_8$. One extreme is to only require that the strongest $C_{10}H_8$ band be present (Salama and Allamandola 1992; Lee and Neff 2007).

For $C_{10}H_8$ (1 mg/L) – Tween 80 (1 mL/L): The spectrum of $C_{10}H_8$-Tween 80 mixture in 96 % ethanol shows two distinct band systems with very different intensities. System I, peaking at 238 nm, is very strong. System II is very weak and peaks at 276 nm. From the obtained results by the full-scan UV detection, we show that the absorption band of $C_{10}H_8$ (1 mg/L) is masked by that of Tween 80 (1 mL/L). Likewise, no effect is observed on the absorption wavelength of Tween 80 (1 mL/L), 238 nm. Fig. 5 shows that with the decrease in the concentration of Tween 80 from 1 mL/L to 10^{-2} mL/L, no absorption band is observed in the UV region. However, the $C_{10}H_8$ (1 mg/L) – Tween 80 (10^{-2} mL/L) full-scan UV detection showed clearly the absorption band of $C_{10}H_8$ at 220 nm, as was shown in Fig. 1. These results have showed that the use of small concentrations of Tween 80 for the flotation of PAHs from PW will not affect the quantification of these organic compounds.

185
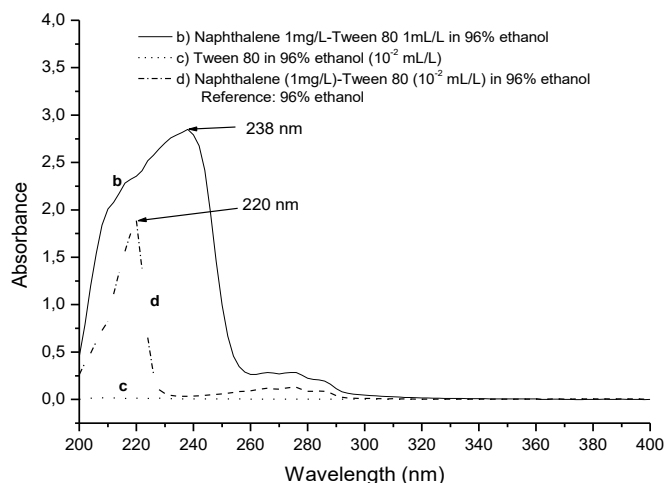
Fig. 5. UV spectra of: b) $C_{10}H_8$ (1 mg/L)-Tween 80 (1 mL/L), c) Tween 80 (10^{-2} mL/L) and d) $C_{10}H_8$ (1 mg/L)-Tween 80 (10^{-2} mL/L) in 96 % ethanol.

Fig. 6. Effect of Tween 80 concentration on the flotation of PAH_{tot}.

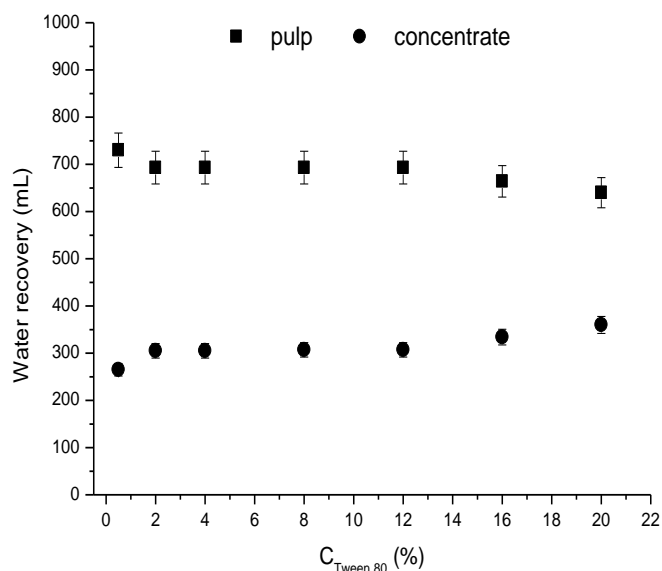*Effect of Tween 80 concentration on the flotation of PAH_{tot}*

The adhesion between PAH molecules and bubbles can be stimulated by adding collectors. Tween 80, used as a non ionic collector, may adsorb onto the surface of the PAHs. In aqueous medium, the hydrophobic effect of the carbon chains of Tween 80 molecules leads to their orientation from water toward the center, forming the core of the micelle with the surface being dominated by the polar hydrophilic groups (Karjiban *et al.* 2012). Thereby, the hydrophobic groups of the free Tween 80 molecules would tend to adsorb on the PAHs surface by reducing the surface tension between PAH-water interfaces. Some PAHs molecules would be trapped within the micelles formed by the Tween 80 molecules and some are attached to the rising bubbles (Mouton *et al.* 2008). The effect of Tween 80 on the recovery of PAH_{tot} from PW was shown in Fig. 6 as a function of concentrations. Flotation tests were carried out at Tween 80 concentrations ranging from 0.5 to 20 %, to recover PAH_{tot} from PW. Ethanol, used as frother, was held constant in all of these tests at test dosage of 0.5 mL/1,000 mL of PW, since it was related that the flotation efficiency is obtained at lower alcohol concentrations (Kowalczuk 2013; Merkus 2016). It was found that frothers not only prevent bubble coalescence, but also, affect the bubble break-up process (Gupta *et al.* 2007). Edzwald (2010) reported that collector-bubble collision efficiency mechanism depends
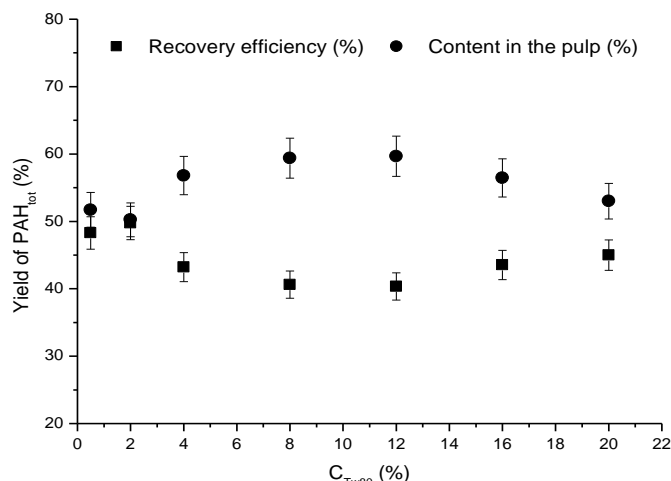
strongly on bubble size, and increases with decreasing bubble size.

Data show that the Tween 80 concentration exhibited a significant effect on the recovery of PAH_{tot} by IAF. The first micelle formed in the flotation cell is introduced as a critical micelle concentration (CMC) (Painmanakul *et al.* 2010). At this concentration, the Tween 80 molecules will start to aggregate and form micelles (Moosai and Dawe 2003; Xu *et al.* 2009). The Tween 80 concentration of 2 % was chosen as the CMC as a result of these experiments for both optimal PAH_{tot} recovery of 49.76 % and PAH_{tot} content in the pulp of 50.24 %. Half of PAHs were removed from PW. Xu *et al.* (2009) reported that the properties of the surfactant vary markedly below and above the CMC. Indeed, at Tween 80 concentration below the CMC, we have observed a decrease in the PAH_{tot} recovery and an increase in the PAH_{tot} content in the pulp. It was reported that a collector at very small quantities is able to change the surface properties of particles, often with little to no influence on any surface properties (Moosai and Dawe 2003). Practically no micelles form below the CMC, the Tween 80 appear as soluble macromolecules in the aqueous medium and cannot interact with PAHs (Baziar *et al.* 2013). Adsorption at the air-water interface is a function of the Tween 80 concentration. The main interactions between Tween 80 and PAHs take place around the CMC. Above the CMC, addition of Tween 80 has no effect on surface tension (Mouton *et al.* 2008).
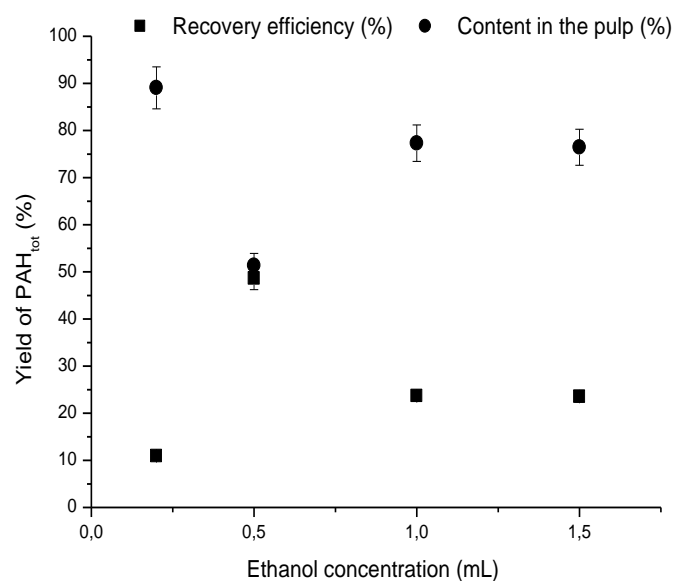
186

Fig. 7. Effect of Tween 80 concentration on water recovery.

Fig. 8. Effect of ethanol concentration on the flotation of PAH_{tot}.

As the Tween 80 concentration was increased above the CMC a trend of decreasing on the PAH_{tot} recovery was observed and at the same time the PAH_{tot} content in the pulp was increased up to the Tween 80 concentration of 12 %. It is well reported that increasing collector concentration leads to an increase in surface adsorption and a corresponding decrease in surface tension (Mouton *et al.* 2008). Indeed, above the CMC, additional Tween 80 molecules added to the pulp will simply form micelles, as this pathway is now energetically favored (Shah *et al.* 2016). Therefore, the surface tension of the liquid phase is essentially constant after the CMC and generally no further PAH molecules will be driven to the surface of the flotation cell up to the Tween 80 concentration above 12 % where we have observed a sudden increase in the PAH_{tot} recovery and decrease in the PAH_{tot} content in the pulp.

The PAHs recovery by IAF is related to the recovery of water. While the primary task is to collect particles, bubbles also transport water. Moyo *et al.* (2007) have reported that the amount of water entrained depends on bubble size. It is known that large bubbles have a high rising velocity, so that the residence time in the flotation cell is shorter (Sawyerr *et al.* 1998; Cho and Laskowski 2002).

Data from Fig. 8 show that the amount of water carried by the bubbles into and through the froth was practically constant from the CMC to 12 % of Tween 80 concentration, and was

increased as the Tween 80 concentration was increased above 12 %. It was also reported that as bubble rise velocity increased, the probability of collision between PAH molecules and bubbles decreased because of the shorter residence time in the flotation cell (Edzwald 2010; Shean and Cilliers 2011). But in this study, we have observed (Fig. 6) that as the Tween 80 concentration was increased above 12 %; the recovery of PAH_{tot} from PW was increased while the PAH_{tot} content in the pulp was decreased. It is believed that the high bubbles rise velocity, from the mixing zone to the froth zone, occurred after a rapid attachment of PAH-Tween 80 aggregates to bubbles in the pulp; these bubbles ascend and form stable froth height at the surface of the flotation cell. With the continuous rising of ascending bubbles, water surrounding the bubbles and in the wake of ascending bubbles continuous to transfer across the pulp/froth interface to the froth and then to the concentrate. Wang *et al.* (2016) have established that there was an increase in the amount of water recovery from the pulp to the froth when increasing impeller speed, especially in the context of high-presence of solid particles. The obtained results (Fig. 7) reveal that there was an increase in the amount of water recovery from the pulp to the concentrate when reaching a certain collector concentration (12 %) above the CMC. This phenomenon leads to the increase in the PAH_{tot} flotation and in the same time affects the concentrate quality.

187
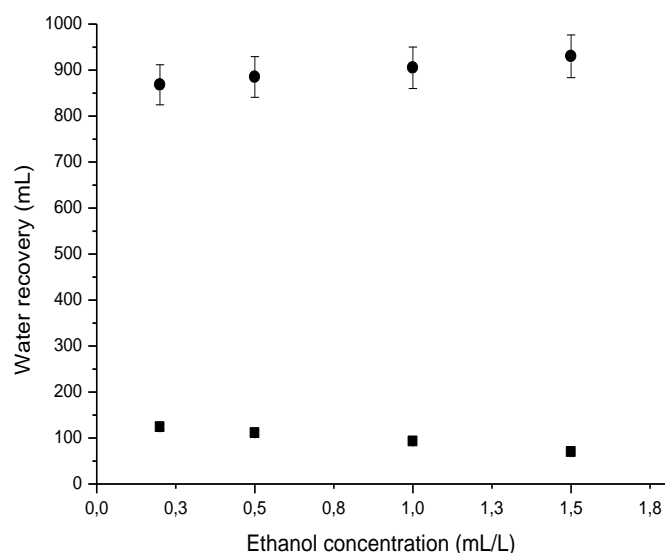
Fig. 9. Effect of ethanol concentration on water recovery. Pulp (circles) and Concentrate (squares) are shown.

Fig. 10. Effect of both CMC and CCC on the flotation of PAH_{tot} at different conditioning times: 5 and 10 min

Effect of ethanol concentration on the flotation of PAH_{tot}

In flotation systems, bubble size is one of the key factors controlling the performance of the process. There is a primary process that generates fine bubbles, and a secondary process that is coalescence. Coalescence requires the out flow of liquid between adjacent bubbles, and as bubble size increases the strength of the water streamline around the bubble increases, making collision between particles and bubbles more difficult. The adsorption of alcohols on the bubble surface retards coalescence and also affects the bubble rise velocity from the mixing zone to the froth zone (Cassel *et al.* 1975; Azgomi *et al.* 2007).

The Fig. 8 gives the flotation of PAH_{tot} at ethanol concentrations varying from 0.2 through 1.5 mL/L. The CMC of Tween 80 was held constant in all of these runs. Ethanol molecules accumulate preferentially at the air-water interface and interact with PAH-Tween 80 aggregates in the PAH-to-bubble collision and attachment.

Data showed that at 0.5 mL/L of ethanol, the optimum PAH_{tot} recovery was about 48.65 % for the PAH_{tot} content in the pulp of 51.35 %. At this concentration, we arrived to recover half of the content of PAH_{tot} in the produced water. This seems to imply that a considerable part of ethanol penetrated effectively into the interfacial film, which stabilizes bubble size in the mixing zone and both increases collision rate with PAH_{tot} molecules
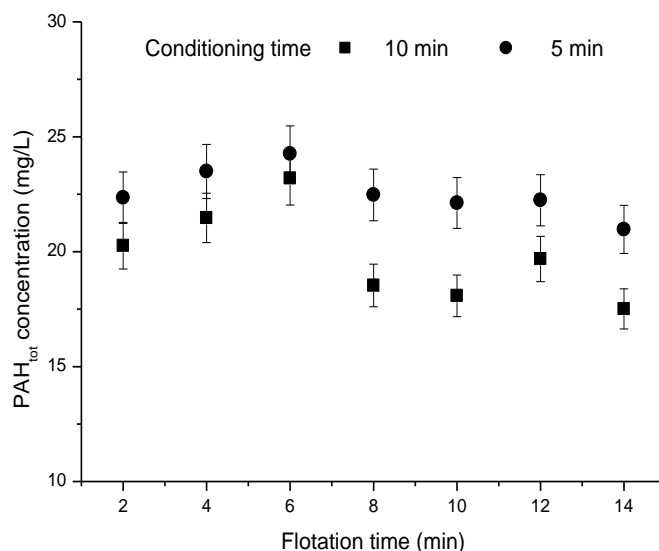
and helps enable stable froth to form, that brings the collected PAH_{tot} to pass into the froth zone and to overflow from the cell. Kowalczuk (2013) reported that bubble size decreases with increasing ethanol amount to a certain concentration, critical coalescence concentration (CCC), above which bubble size remains approximatively constant, and at the CCC bubble coalescence is completely prevented. According to these results, the CCC of ethanol was of 0.5 mL/L.

Above the CCC, we noticed the decrease in the PAH_{tot} recovery from PW and simultaneously an increase in the PAH_{tot} content in the pulp. Cheng *et al.* (2016) related that when bubbles are too small, particles may have insufficient contact time to attach to the bubbles, or if attachment does occur, the bubbles buoyancy may be low for considerable recovery. Effectively, above the CCC, the recovery of PAH_{tot} is lower and approximatively constant, 23.69 and 23.55 % for 1 mL/L and 1.5 mL/L, respectively. Furthermore, the PAH_{tot} content in the pulp is higher and approximatively constant. This means that the PAH-bubble attachment was occurred, but because of the constant bubble size, the very low bubble rise velocity from the mixing zone to the froth zone the PAH_{tot} recovery was low.

Below the CCC, the PAH_{tot} recovery was not important (10.95 %), and the PAH_{tot} content in the pulp was higher (89.05 %). This can be explained by the fact that smallest concentration of ethanol didn't prevented coalescence and therefore large

188
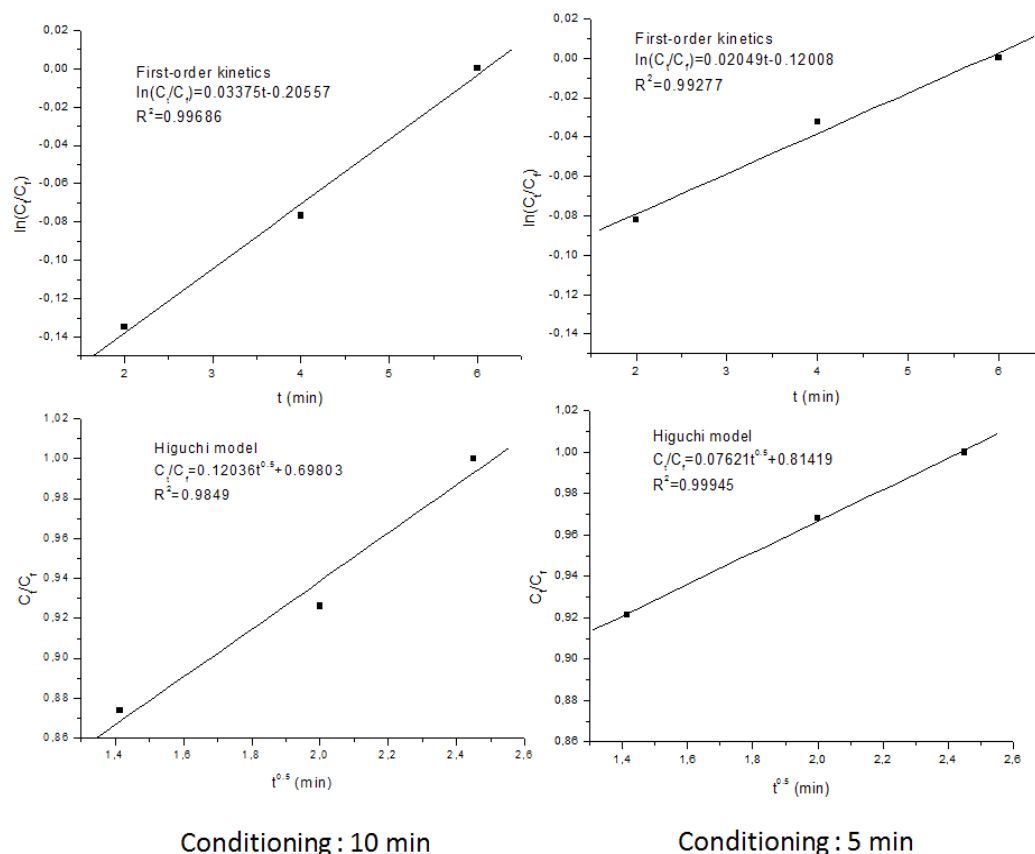
Fig. 11. Effect of both CMC and CCC on the flotation kinetics of PAH$_{tot}$ at different conditioning times as a function of concentration.

bubbles were formed and bubble rise velocity was higher, because of these, the possibility of collision between bubbles and PAH molecules is decreased. Data from Fig. 9 show that the amount of water carried by the bubbles from the pulp to the concentrate was decreased as the ethanol concentration was increased. Moyo *et al.* (2007) have established that the adsorption of alcohol on the bubble surface leads to the transport of less water into the froth.

In this study, little amounts of water were carried by bubbles into the concentrate at all ethanol concentrations. Gupta *et al.* (2007) believed that the continued addition of ethanol above the CCC must leads to a very little effect on bubble size which leads automatically, in the same conditions, to a probable fixed amounts of water recovery. However, in this study, we have observed that, despite the increase on ethanol concentration above the CCC, the amount of water recovery into was decreased. This is probably related to the impact of the high-presence of PAH molecules (Fig. 8) on the water flow in the froth.

Effect of both CMC and CCC on the flotation kinetics of PAH$_{tot}$

The obtained results were presented to study the effect of both CMC and CCC on the flotation of PAH$_{tot}$ at different conditioning times: 5 and 10 min (Fig. 10). The results showed for the two different conditioning times a high flotation of PAH$_{tot}$ from PW during the initial 6 min, and then a decrease followed by stabilization.

The concentration of PAH$_{tot}$ increases with flotation time and approached an asymptote. It can be noted that the increase in PAH$_{tot}$ concentration of was marginal if the flotation time was extended beyond 6 min. Hence, 6 min may be considered as the optimal flotation time of PAH$_{tot}$.

Addition of both Tween 80 and ethanol at the CMC and the CCC, respectively, significantly increased the kinetics of flotation of PAH$_{tot}$. It can be seen that the presence of Tween 80 and ethanol at these concentrations has lead to the decrease in both flotation time of PAH$_{tot}$ from 20 to 6 min and conditioning time from 30 to 10 min (Chebbi *et al.* 2016) for the two conditioning times.

189

The formation of the froth and its subsequent removal are the final two steps in flotation. Phenomena that occur in the froth phase are known to affect significantly the results of the whole process. The concentration of PAHs in the uppermost pulp layers is of interest. Above 6 min of flotation, PAH_{tot} molecules fall dawn in the bottom of the flotation cell and then stabilize until the end of the process. This behavior might be because of a change in froth structure caused by variation in the flotation of PAHs from the pulp to the concentrate. Furthermore, for a fixed flotation reagents concentrations (CMC and CCC), micelle concentration and bubble size were fixed, and since the impeller speed and the air flow rate were also kept fixed in this study, the flotation of PAH_{tot} was limited even though the flotation time has considerably decreased. Fig. 11 shows a linearization of the flotation of PAH_{tot} according to the concentration for each supposed kinetics model. The following concentrations were evaluated for each conditioning time: 5 and 10 min. The data was plotted for comparison. It can be seen that the Higuchi model showed a higher flotation rates of 0.07621 and 0.12036 min^{-1} over time for the conditioning times of 5 and 10 min, respectively. Since, the first-order kinetics showed a slower flotation rates over time of 0.02049 and 0.03375 min^{-1} for the conditioning times of 5 and 10 min, respectively.

The two supposed kinetics models assumes that the PAH-bubble collision rate and bubble concentration remain constant over time. Higuchi model for PAH/water separation by IAF has also been found by the previous work (Chebbi *et al.* 2016), and the optimal conditioning time in this study and under these operational conditions was found to be around 10 min as has been illustrated by the flotation rate of 0.12036 min^{-1}.

Conclusions

According to the results, the binary solvent (water-ethanol) and Tween 80 failed to destabilize the molecular orbital of naphthalene. The use of two or one of the solvents as reference to quantify PAH_{tot} had no effect the analysis. The use of Tween 80 at small concentrations has been proven discrete in the quantification of PAH_{tot}. It's presence with lower concentrations promoted the flotation of PAHs. The maximum flotation of PAH_{tot} was observed at the CMC of 2 % with a recovery of 49.76 % and a content in the pulp of 50.24 %. At this concentration, half of PAH_{tot} were removed. Since the impeller speed and air flow rate were constant, the flotation of PAHs was limited. The water carrying begins to become an undesirable product in the recovery of oil when it reaches a certain amount. Above the CMC, large amounts of water were carried. Therefore, PAH_{tot} recovery decreased and PAH_{tot} content in the PW increased. It was found that at a certain concentration of Tween 80 (12 %), far above the CMC, the PAH_{tot} recovery start to increase and PAH_{tot} content in the PW to decrease. This phenomenon can mislead researcher about the CMC value. Addition of ethanol greatly promote the flotation of PAHs, the CCC was found to be around 0.5 mL/L. Contrary to the CMC, the increase in the ethanol concentration at the CMC, above the CCC, has decreased the water recovery. The kinetics experiment on the effect of both CMC and CCC on the flotation process has showed that at these operational conditions the conditioning time was decreased from 30 to 10 min, while the flotation time was decreased from 20 to 6 min as found in the previous work. It was found that the flotation kinetics of PAH_{tot} was governed by the Higuchi model.

Acknowledgements

References

Akinwumi A (2013) Rheological effect of produced water on crude oil flow in production tubing string: a case study of agbami oil field, Nigeria. Int. J. Sci. Res. 2: 229-233.

Alanezi K, Belkharchouch M, Alali S, Abuhaimed W (2013) Produced water characterization in Kuwait and its impact on the environment. Desalin. Water Treat. 51: 302-306.

Almeda R, Wambaugh Z, Chai C, Wang Z, Liu Z, Buskey EJ (2013) Effects of crude oil exposure on bioaccumulation of polycyclic aromatic hydrocarbons and survival of adult and larval stages of gelatinous zooplankton. PloS one 8: e74476.

Azgomi F, Gomez CO, Finch JA (2007) Correspondence of gas holdup and bubble size in presence of different frothers. Int. J. Min. Process. 83: 1-11.

Baziar M, Mehrasebi MR, Assadi A, Fazli MM, Maroosi M, Rahimi F (2013) Efficiency of non-ionic surfactants - EDTA for treating TPH and heavy metals from contaminated soil. J. Environ. Health Sci. Eng. 11: 1-6.

Bournival G, de Oliveira e Souza L, Ata S, Wanless EJ (2015) Effect of alcohol frothing agents on the coalescence of bubbles coated with hydrophobized silica particles. Chem. Eng. Sci. 131: 1-11.

Cassel EA, Kaufman MK, Matijevic E (1975) The effects of bubble size on microflotation. Water Res. 9: 1017-1024.

Chebbi S, Belkacemi H, Merabet D (2016) Physicochemical characterization and kinetic study of flotation process applied to the treatment of produced water. J. Environ. Anal. Toxicol. 6: 362.

Cheng G, Shi CL, Liu JT, Yan XK (2016) Bubble-distribution measurement in a flotation column. Int. J. Coal Prep. Util. 36: 241-250.

Cho YS, Laskowski JS (2002) Effect of flotation frothers on bubble size and foam stability. Int J Miner Process 64: 69-80.

Crawford MK, Tielens AGGM, Allamandola LJ (1985) Ionized polycyclic aromatic hydrocarbons and the diffuse interstellar bands. Astrophys. J. 293: 45-48.

Edwan K, Qomarudin H (2015) Petroleum oil and gas industry waste treatment; common practice in Indonesia. J. Pet. Environ. Biotechnol. 6: 241.

Edzwald JK (2010) Dissolved air flotation and me. Water Res. 44: 2077-2106.

El-Kayar A, Hussein M, Zatout AA, Hosny AY, Amer AA (1993) Removal of oil from stable oil-water emulsion by induced air flotation technique. Sep. Technol. 3: 25-31.

Fisner M, Taniguchi S, Moreira F, Bicego MC, Turra A (2013) Polycyclic aromatic hydrocarbons (PAHs) in plastic pellets: variability in the concentration and composition at different sediment depths in a sandy beach. Mar. Pollut. Bull. 70: 219-226.

Gharibzadeh F, Rezaei Kalantary R, Nasseri S, Esrafili A, Azari A (2016) Reuse of polycyclic aromatic hydrocarbons (PAHs) contaminated soil washing effluent by bioaugmentation/biostimulation process. Sep. Purif. Technol. 168: 248-256.

Gupta AK, Banerjee PK, Mishra A, Satish P, Pradip (2007) Effect of alcohol and polyglycol ether frothers on foam stability, bubble size and coal flotation. Int. J. Min. Process. 82: 126-137.

Hagström EL, Lyles C, Pattanayek M, DeShields B, Berkman MP (2016) Produced water – emerging challenges, risks, and opportunities. Environ. Claims J. 28: 122-139.

Hoseini SM, Salarirad MM, Alavi Moghaddam MR (2013) TPH removal from oily wastewater by combined coagulation pretreatment and mechanically induced air flotation. Desalin. Water Treat. 53: 300-308.

Karjiban RA, Basri M, Rahman MBA, Salleh AB (2012) Structural properties of nonionic Tween80 micelle in water elucidated by molecular dynamics simulation. APCBEE Procedia 3: 287-297.

Kowalczuk PB (2013) Determination of critical coalescence concentration and bubble size for surfactants used as flotation frothers. Ind. Eng. Chem. Res. 52: 11752-11757.

Lau EV, Foo KL, Poh PE (2013) The recovery of oil from oil/sand slurries in a laboratory-scale flotation cell. Int. J. Environ. Sci. Develop. 4: 351-354.

Lau EV, Gan S, Ng HK, Poh PE (2014) Extraction agents for the removal of polycyclic aromatic hydrocarbons (PAHs) from soil in soil washing technologies. Environ. Pollut. 184: 640-649.

Lee K, Neff J (2007) Abstracts of the international produced water conference: environmental risks and advances in mitigation technologies. St. John´s Newfoundland, Canada, October 17-18, National energy board of Canada, Environmental Studies Research Fund (ESRF).

Lee K, Neff J (2011) Produced water: environmental risks and advances in mitigation technologies, Springer, New York, USA, 608 p.

Li P, Tsuge H (2006) Water tratment by induced air flotation using microbubbles. J. Chem. Eng. Japan 39: 896-903.

Merkus HG (2016) Flotation. In Merkus HG, Meesters GMH (Eds.), Production, handling and characterization of particulate materials, Springer International Publishing, Particle Technology Series, Vol 25. Springer, Cham, pp. 389-405.

Mistry BD (2009) Chemistry (UV, JR, PMR, JJCNMR and Mass Spectroscopy), A Handbook of Spectroscopic Data, 240 p.

Monakhova YB, Astakhov SA, Kraskov A, Mushtakova SP (2010) Independent components in spectroscopic analysis of complex mixtures. Chemometr. Intell. Lab. 103: 108-115.

Moosai R, Dawe RA (2003) Gas attachment of oil droplets for gas flotation for oily wastewater cleanup. Sep. Purif. Technol. 33: 303-314.

Mouton J, Mercier G, Blais J-F (2008) Amphoteric surfactants for PAH and lead polluted-soil treatment using flotation. Water Air Soil Pollut. 197: 381-393.

Moyo P, Gomez CO, Finch JA (2007) Characterizing frothers using water carrying rate. Can. Metall. Q. 46: 215-220.

Ofori P, O'Brien G, Firth B, McNally C (2012) The use of tri-block copolymer surfactants as promoters to improve flotation recovery of poorly floating coal components. Int. J. Coal Prep. Util. 32: 103-119.

Painmanakul P, Sastaravet P, Lersjintanakarn S, Khaodhiar S (2010) Effect of bubble hydrodynamic and chemical dosage on treatment of oily wastewater by Induced Air Flotation (IAF) process. Chem. Eng.Res. Des. 88: 693-702.

Pardue MJ, Castle JW, Rodgers JH Jr, Huddleston GM 3rd (2014) Treatment of oil and grease in produced water by a pilot-scale constructed wetland system using biogeochemical processes. Chemosphere 103: 67-73.

Ramaswamy B, Kar DD, De S (2007) A study on recovery of oil from sludge containing oil using froth flotation. J. Environ. Manage. 85: 150-154.

Roodbari NH, Badiei A, Soleimani E, Khaniani Y (2016) Tweens demulsification effects on heavy crude oil/water emulsion. Arab. J. Chem. 9: S806-S811.

Salama F, Allamandola LJ (1992) The ultraviolet and visible spectrum of the polycyclic aromatic hydrocarbon $C_{10}H_8^+$: possible contributions to the diffuse interstellar bands and to the ultraviolet-visible extinction. Astraphys. J. 395: 301-306.

Salama F, Allamandola LJ (1993) Neutral and ionized polycyclic aromatic hydrocarbons, diffuse interstellar bands and the ultraviolet extinction curve. J. Chem. Soc., Faraday Trans. 89: 2277-2284.

Salama F, Allamandola LJ (1995) Polycyclic aromatic hydrocarbon ions and the diffuse interstellar bands. Adv. Space Res. 15: 413-422.

Sawyerr F, Deglon DA, O'Connor CT (1998) Prediction of bubble size distribution in mechanical flotation cells. J. South Afr. Inst. Min. Metall. 98: 179-186.

Shah A, Shahzad S, Munir A, Nadagouda MN, Khan GS, Shams DF, Dionysiou DD, Rana UA (2016) Micelles as soil and water decontamination agents. Chem. Rev. 116: 6042-6074.

Shean BJ, Cilliers JJ (2011) A review of froth flotation control. Int. J. Min. Process. 100: 57-71.

Siepmann J, Peppas NA (2011) Higuchi equation: derivation, applications, use and misuse. Int. J. Pharm. 418: 6-12.

Sylvester ND, Byeseda JJ (1980) Oil/water separation by induced-air flotation. SSPE J. 20: 579-590.

Szymczyk K, Taraba A (2016) Aggregation behavior of Triton X-114 and Tween 80 at various temperatures and concentrations studied by density and viscosity measurements. J. Therm. Anal. Calorim. 126: 315-326.

Wang L, Runge K, Peng Y (2016) The observed effect of flotation operating conditions and particle properties on water recovery at laboratory scale. Min. Eng. 94: 83-93.

Wang LK, Shammas NK, Selke WA, Aulenbach DB (2010) Flotation technology, Humana Press, c/o Springer Science + Business Media 12, 680 p.

Weide T, Guschin V, Becker W, Koelle S, Maier S, Seidelt S (2015) Analysis of pure tar substances (polycyclic aromatic hydrocarbons) in the gas stream using ultraviolet visible (UV-Vis) spectroscopy and multivariate curve resolution (MCR). Appl. Spectrosc. 69: 143-153.

Wuelfing WP, Kosuda K, Templeton AC, Harman A, Mowery MD, Reed RA (2006) Polysorbate 80 UV-vis spectral and chromatographic characteristics – defining boundary conditions for use of the surfactant in dissolution analysis. J. Pharm. Biomed. Anal. 41: 774-782.

Xu Q, Nakajima M, Ichikawa S, Nakamura N, Roy P, Okadome H, Shiina T (2009) Effects of surfactant and electrolyte concentrations on bubble formation and stabilization. J. Colloid. Interface. Sci. 332: 208-214.

Zheng YY, Zhao CC (1993) A study of kinetics on induced-air flotation for oil-water separation. Sep. Sci. Technol. 28: 1233-1240.